PROCEEDINGS OF SCIENCE

$\bar{b}\bar{b}ud$ Tetraquark Resonances in the Born-Oppenheimer Approximation using Lattice QCD Potentials

M. Pflaumer[*],[a] **P. Bicudo,**[b] **M. Cardoso,**[b] **A. Peters,**[a] **and M.Wagner** [a]

[a]*Goethe-Universität Frankfurt am Main, Institut für Theoretische Physik, Max-von-Laue-StraÃ§e 1, D-60438 Frankfurt am Main, Germany*

[b] *CeFEMA, Instituto Superior Técnico, Universidade de Lisboa, Av. Rovisco Pais, 1049-001 Lisboa, Portugal*

E-mail: pflaumer@th.physik.uni-frankfurt.de, bicudo@tecnico.ulisboa.pt, mjdcc@cftp.ist.utl.pt, peters@th.physik.uni-frankfurt.de, mwagner@th.physik.uni-frankfurt.de

We study tetraquark resonances for a pair of static antiquarks $\bar{b}\bar{b}$ in presence of two light quarks ud based on lattice QCD potentials. The system is treated in the Born-Oppenheimer approximation and we use the emergent wave method. We focus on the isospin $I = 0$ channel but take different angular momenta l of the heavy antiquarks $\bar{b}\bar{b}$ into account. Further calculations have already predicted a bound state for the $l = 0$ case with quantum numbers $I(J^P) = 0(1^+)$. Performing computations for several angular momenta, we extract the phase shifts and search for T and S matrix poles in the second Riemann sheet. For angular momentum $l = 1$, we predict a tetraquark resonance with quantum numbers $I(J^P) = 0(1^-)$, resonance mass $m = 10576^{+4}_{-4}$ MeV and decay width $\Gamma = 112^{+90}_{-103}$ MeV, which decays into two B mesons.

XIII Quark Confinement and the Hadron Spectrum - Confinement2018
31 July - 6 August 2018
Maynooth University, Ireland

[*]Speaker.

PoS(Confinement2018)123

1. Introduction

A very challenging problem in particle physics is understanding exotic hadrons. In this work, we investigate a tetraquark system with two heavy antiquarks $\bar{b}\bar{b}$ and two light quarks qq with $q \in \{u,d,s,c\}$. While the existence of bound states has been studied in recent years applying lattice QCD potentials and the Born-Oppenheimer approximation, a stable tetraquark state has been predicted with quantum numbers $I(J^P) = 0(1^+)$ [1, 2, 3, 4, 5, 6, 7, 8, 9]. This state has been confirmed using heavy quarks of finite mass [10]. The current work extends this investigation by a new technique from scattering theory, the emergent wave method [11], and we search for possibly existing tetraquark resonances (cf. [12]).

2. Lattice QCD Potentials of two Static Heavy Antiquarks $\bar{Q}\bar{Q}$ in the Presence of two Light Quarks qq

In previous studies, we have computed the potentials $V(r)$ for two static antiquarks $\bar{Q}\bar{Q}$ in the presence of two light quarks qq applying methods of lattice QCD. Calculations have been performed for different light quark flavour combinations i.e. qq with $q \in \{u,d,s,c\}$. Moreover, several values for the parity P and the total angular momentum of the light quarks and gluons j (cf. e.g. [7, 8]) have been studied. For these wide range of quantum numbers, there are attractive as well as repulsive channels. There have been identified two attractive potentials with $q \in \{u,d\}$ which are quite wide and deep. These are most promising when investigating the existence of bound tetraquark states or resonances. The two attractive potentials are characterised by the quantum numbers ($I = 0, j = 0$) and ($I = 1, j = 1$). The potentials are illustrated in Fig. 1 for lattice spacing $a \approx 0.079$ fm and u/d quark masses corresponding to a pion mass $m_\pi \approx 340$ MeV.
It is well-known, that the binding energy and hence the existence or non-existence of a stable tetraquark state depends on the light quark mass [7]. Thus, we have performed calculations for three different light quark masses u/d corresponding to $m_\pi \in \{340\,\text{MeV}, 480\,\text{MeV}, 650\,\text{MeV}\}$. These results are used to perform an extrapolation to $m_\pi = 140\,\text{MeV}$. Moreover, a study of discretisation errors and final volume effects shows that these uncertainties are negligible compared to statistical uncertainties (cf. [8]). Searching for bound states as well as resonances, we parametrize the

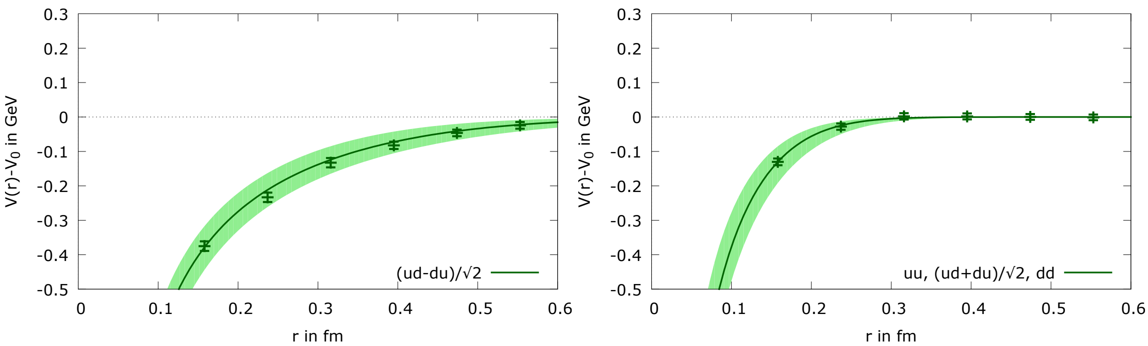

Figure 1: (left) ($I = 0, j = 0$) potential. (right) ($I = 1, j = 1$) potential.

potential by a screened Coulomb potential:

$$V(r) = -\frac{\alpha}{r} e^{-r^2/d^2}. \tag{2.1}$$

This ansatz is motivated by a one-gluon exchange for small $\bar{Q}\bar{Q}$ separations r and the formation of

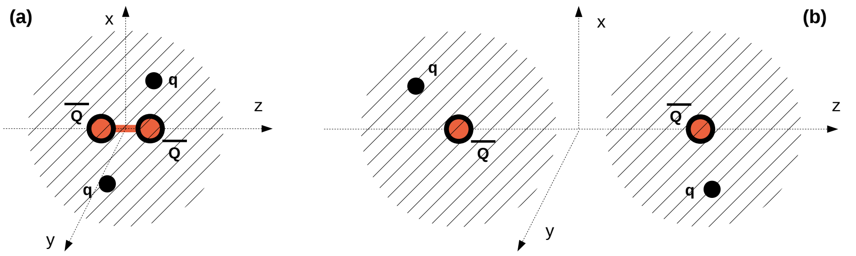

Figure 2: (a) At small separations the static antiquarks $\bar{Q}\bar{Q}$ interact by perturbative one-gluon exchange. (b) At large separations the light quarks qq screen the interaction and the four quarks form two rather weakly interacting B mesons.

two B mesons at larger r as a consequence of a screened Coulomb potential (cf. Fig. 2). Even if this approach is phenomenologically motivated, it is consistence with our lattice QCD results.
The numerical results for the parameters α and d are listed in Table 1. Clearly, the $(I = 0, j = 0)$ potential is more attractive than the $(I = 1, j = 1)$ potential. Consequently, Eq. (2.1) describes the

I	j	α	d in fm
0	0	$0.34^{+0.03}_{-0.03}$	$0.45^{+0.12}_{-0.10}$
1	1	$0.29^{+0.05}_{-0.06}$	$0.16^{+0.05}_{-0.02}$

Table 1: Parameters α and d of the potential of Eq. (2.1) for two static antiquarks $\bar{Q}\bar{Q}$, in the presence of two light quarks qq with quantum numbers I and j, as determined in [8]

potential of two heavy antiquarks $\bar{b}\bar{b}$ in the presence of two light quarks ud, so in other words, we apply a Born-Oppenheimer approximation [13]. We can use this potential in the Schrödinger equation to search for either bound states (cf. [5, 7, 9, 12]) or resonances (cf. Sec. 3 and 4). Solving the Schrödinger equation for $(I = 0, j = 0)$, a bound state with binding energy 90^{+43}_{-36} MeV and quantum numbers $I(J^P) = 0(1^+)$ has been found [8].

3. The Emergent Wave Method

In this section, we present the emergent wave method, which is a well suited approach to study phase shifts and resonances. More details can be found, for example, in [11]. First, we consider the well-known Schrödinger equation

$$\Big(H_0 + V(r)\Big)\Psi = E\Psi . \tag{3.1}$$

We start by splitting the wave function into two parts,

$$\Psi = \Psi_0 + X \ , \tag{3.2}$$

where Ψ_0 is the incident wave, which solves the free Schrödinger equation $H_0\Psi_0 = E\Psi_0$ and X indicates the emergent wave. As the next step, we insert Eq. (3.2) into Eq. (3.1) . Using the free Schrödinger equation to simplify, we obtain:

$$\Big(H_0 + V(r) - E\Big)X = -V(r)\Psi_0 \ . \tag{3.3}$$

Solving this equation for any arbitrary energy E, we can compute the emergent wave X by providing the corresponding Ψ_0 and fixing the appropriate boundary conditions. The asymptotic behaviour of X determines the phase shifts, the S matrix and the T matrix. Continuing this problem to complex energies is possible without difficulties. We find the poles of the S matrix and the T matrix in the complex plane and identify them with a resonance, when located in the second Riemann sheet at $m - i\Gamma/2$, where m is the mass and Γ is the decay width of the resonance.

3.1 Partial Wave Decomposition

The Hamiltonian describing the two heavy antiquarks $\bar{b}\bar{b}$ at vanishing total momentum is

$$H = H_0 + V(r) = -\frac{\hbar^2}{2\mu}\triangle + V(r) \tag{3.4}$$

where $\mu = M/2$ is the reduced mass and $M = 5280\,\text{MeV}$ is the mass of the B meson from the PDG [14]. We consider all results as energy differences with respect to $2M$, so we omit the additive constant $2M$ in Eq. (3.4). In the next step, we express the incident plane wave $\Psi_0 = e^{i\mathbf{k}\cdot\mathbf{r}}$ as a sum of spherical waves,

$$\Psi_0 = e^{i\mathbf{k}\cdot\mathbf{r}} = \sum_l (2l+1)i^l j_l(kr)P_l(\hat{\mathbf{k}}\cdot\hat{\mathbf{r}}) \ , \tag{3.5}$$

where j_l are spherical Bessel functions, P_l are Legendre polynomials and the relation between energy and momentum is $\hbar k = \sqrt{2\mu E}$. Since the potential $V(r)$ in Eq. (2.1) is spherically symmetric, we can also expand the emergent wave X in terms of Legendre polynomials P_l,

$$X = \sum_l (2l+1)i^l \frac{\chi_l(r)}{kr} P_l(\hat{\mathbf{k}}\cdot\hat{\mathbf{r}}) \ . \tag{3.6}$$

Inserting Eq. (3.5) and Eq. (3.6) into Eq. (3.3) leads to a set of ordinary one-dimensional differential equations for χ_l,

$$\left(-\frac{\hbar^2}{2\mu}\frac{d^2}{dr^2} + \frac{l(l+1)}{2\mu r^2} + V(r) - E\right)\chi_l(r) = -V(r)kr\,j_l(kr) \ . \tag{3.7}$$

3.2 Solving the Differential Equations for the Emergent Wave

The potentials $V(r)$, Eq. (2.1), are exponentially screened, i.e. $V(r) \approx 0$ for $r \geq R$, where $R \gg d$. Consequently, the emergent wave is a superposition of outgoing spherical waves for large separations $r \geq R$ and can be expressed by the spherical Hankel functions of first kind $h_l^{(1)}$:

$$\frac{\chi_l(r)}{kr} = i t_l h_l^{(1)}(kr). \tag{3.8}$$

If we compute the complex prefactors t_l, this will lead to the phase shifts. To this end we solve the ordinary differential equation (3.7) with the corresponding boundary conditions as follows:

- At $r = 0$: $\chi_l(r) \propto r^{l+1}$.
- For $r \geq R$: Eq. (3.8).

We emphasize that the boundary condition for $r \geq R$ depends on t_l. Solving the differential equation for a given value of the energy E, this boundary condition is only fulfilled for a specific corresponding value of t_l. In other words the boundary condition for $r \geq R$ fixes t_l as a function of E.

For the numerical solution of Eq. (3.7), we implement two different and independent approaches:

(1) A fine uniform discretization of the interval $[0,R]$, which reduces the differential equation to a large set of linear equations, which can be solved rather efficiently, since the corresponding matrix is tridiagonal;

(2) A standard 4-th order Runge-Kutta shooting method.

3.3 Phase Shifts, S and T Matrix Poles

We identify t_l as an eigenvalue of the T matrix (cf. standard textbooks on quantum mechanics and scattering, e.g. [15]). Knowing t_l we can determine the phase shift δ_l and also the corresponding S matrix eigenvalue s_l [1],

$$s_l \equiv 1 + 2it_l = e^{2i\delta_l} \; . \tag{3.9}$$

Note that both the S matrix and the T matrix are analytical in the complex plane and are also well-defined for complex energies E. Thus, we extend our numerical method to solve the differential Eq. (3.7) to complex E and detect the S and T matrix poles by scanning the complex plane $(\mathrm{Re}(E), \mathrm{Im}(E))$ and applying Newton's method to find the roots of $1/t_l(E)$. These poles correspond to complex energies of resonances and must be located in the second Riemann sheet with a negative imaginary part both for the energy E and the momentum k.

4. Results for the Phase Shifts, S- and T-Matrix Poles and Prediction of Resonances

4.1 Phase Shifts δ_l for Real Energies E

First, we consider the more attractive channel ($I = 0, j = 0$) of the $\bar{b}\bar{b}ud$ potential (cf. Sec 2). We compute t_l for real energies E and apply Eq. (3.9) to determine the phase shift δ_l for the different angular momenta $l = 0, 1, 2, 3, \ldots$. For a resonance, we expect a fast increasing of δ_l from 0 to $\approx \pi$ which is, however, not clearly found (cf. Fig. 3 (left)). Thus, we have to search more thoroughly if there exists a resonance or not. We consider the $l = 1$ channel and search for a clear resonance making the potential more attractive by increasing the parameter α while d is kept fixed. We illustrate the phase shifts δ_1 in Fig. 3 (right). For $\alpha \gtrsim 0.65$ we find a clear resonance while for $\alpha = 0.72$ a bound state is formed, i.e. the phase shift starts at π and decreases monotonically. However, this observation does not allow to make a clear statement for which values of α a resonance exists or not.

[1] At large distances $r \geq R$, the radial wavefunction is $kr[j_l(kr) + it_l h_l^{(1)}(kr)] = (kr/2)[h_l^{(2)}(kr) + e^{2i\delta_l} h_l^{(1)}(kr)]$.

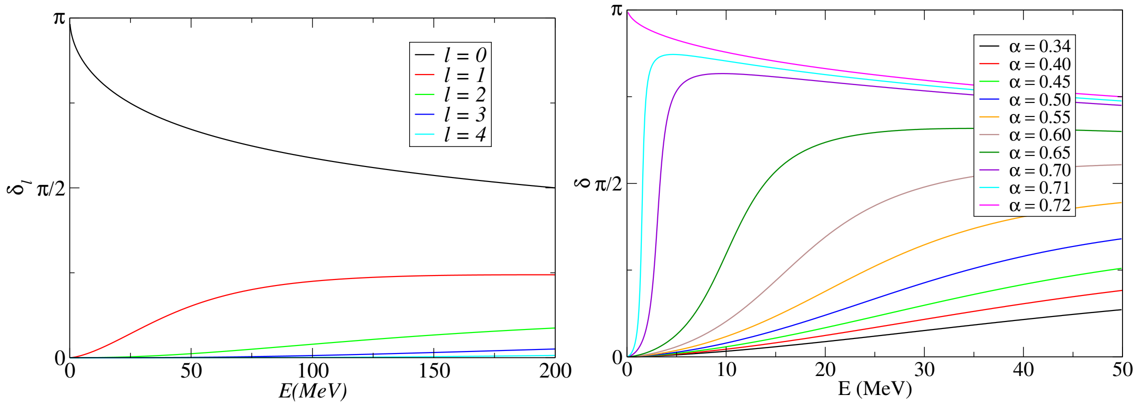

Figure 3: **(left):** Phase shift δ_l as a function of the energy E for different angular momenta $l = 0,1,2,3,4$ for the $(I = 0, j = 0)$ potential ($\alpha = 0.34$, $d = 0.45\,\mathrm{fm}$). **(right):** Phase shift δ_1 as a function of the energy E for different parameters for the potential. For illustration, we vary parameter α only while fixing $d = 0.45\,\mathrm{fm}$ at the value of the $(I = 0, j = 0)$ potential. Fixing d and varying α produces comparable results.

4.2 Resonances as Poles of the S and T Matrices for Complex Energies E

Thus, we search directly for resonances as poles of the T matrix eigenvalue t_l in the complex energy plane. For angular momentum $l = 1$ and the physical $(I = 0, j = 0)$ potential, we clearly identify a pole which is shown in Fig. 4 (left) plotting t_1 as a function of the complex energy E. For a better understanding of the resonance and its dependence on the potential, we determine the pole of the T matrix eigenvalue t_l for various parameters α. In Fig. 4 (right), we illustrate the location of the pole for different values of α in the $(\mathrm{Re}(E), \mathrm{Im}(E))$ plane. Indeed, starting with $\alpha = 0.21$ we find poles. Consequently, our prediction for a resonance at $\alpha = 0.34$ is confirmed. For angular momenta $l \neq 1$ as well as for the less attractive channel $(I = 1, j = 1)$ for all l, no pole has been found.

4.3 Statistical and Systematic Error Analysis

Finally, we perform a detailed statistical and systematic error analysis with regard to the pole of t_1 in the complex plane $(\mathrm{Re}(E), \mathrm{Im}(E))$ for angular momentum $l = 1$. We apply the same analysis methods as for our study of bound states presented in [7]. We parametrize the lattice QCD data for the potential $V^{\mathrm{lat}}(r)$ with an uncorrelated χ^2 minimizing fit with the ansatz of Eq. (2.1), i.e. we minimize the expression

$$\chi^2 = \sum_{r=r_{\min},\ldots,r_{\max}} \left(\frac{V(r) - V^{\mathrm{lat}}(r)}{\Delta V^{\mathrm{lat}}(r)} \right)^2 \tag{4.1}$$

with respect to α and d defined in Eq. (2.1). $\Delta V^{\mathrm{lat}}(r)$ denotes the corresponding statistical errors.

To investigate systematic errors, we perform fits for various fit ranges. Besides, we vary the range of the temporal separation $t_{\min} \le t \le t_{\max}$ of the correlation function where $V^{\mathrm{lat}}(r)$ is read off and the spatial separation $r_{\min} \le r \le r_{\max}$ denoting the $\bar{b}\bar{b}$ distance considered in the χ^2 minimizing fit to determine the parameters α and d.

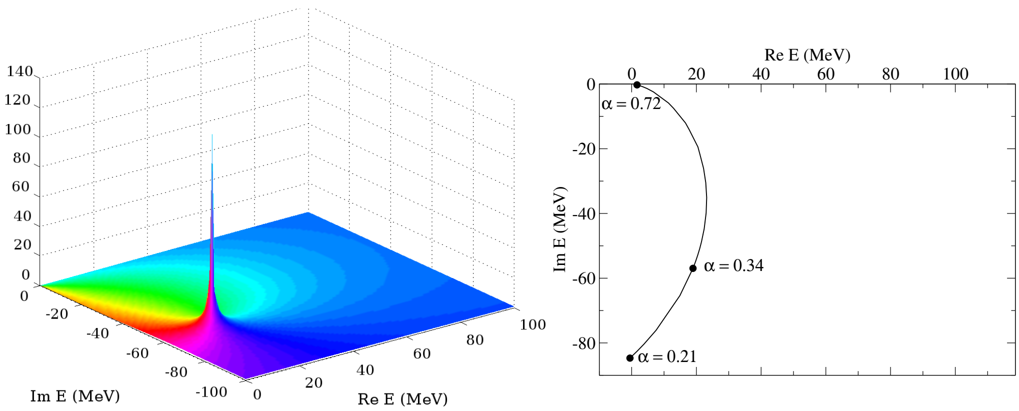

Figure 4: **(left):** T matrix eigenvalue t_1 as a function of the complex energy E for the $(I=0, j=0)$ potential ($\alpha = 0.34$, $d = 0.45\,\mathrm{fm}$). Along the vertical axis we show the norm $|t_1|$, while the phase $\arg(t_l)$ corresponds to different colours. **(right):** Trajectory of the pole of the eigenvalue t_1 of the T matrix in the complex plane $(\mathrm{Re}(E), \mathrm{Im}(E))$, corresponding to a variation of parameter. We also illustrate with a cloud of diamond points the systematic error [7].

The statistical errors are included determining the jackknife errors of the medians of $\mathrm{Re}(E)$ and $\mathrm{Im}(E)$. Finally, systematic and statistical uncertainties are added quadratically.

Applying this combined systematic and statistical error analysis, we find a resonance energy $\mathrm{Re}(E) = 17^{+4}_{-4}\,\mathrm{MeV}$ and a decay width $\Gamma = -2\mathrm{Im}(E) = 112^{+90}_{-103}\,\mathrm{MeV}$. Studying the symmetries of the quarks with respect to colour, flavour, spin and their spatial wave function and considering the Pauli principle we determine the quantum numbers to be $I(J^P) = 0(1^-)$. The decay product of this resonance will be two B mesons, so its mass is given by $m = 2M + \mathrm{Re}(E) = 10576^{+4}_{-4}\,\mathrm{MeV}$.

5. Conclusion and Outlook

We searched for resonances in the $\bar{b}\bar{b}ud$ system applying lattice QCD potentials for two static antiquarks in the presence of two light quarks, the Born-Oppenheimer approximation and the emergent wave method. First, we have considered the scattering phase shift for a BB meson pair. Afterwards, we continued analytically the S matrix and T matrix to the second Riemann sheet and searched for poles in the complex plane.

After a solid statistical and systematic analysis, we predict a new resonance with quantum numbers $I(J^P) = 0(1^-)$, a resonance mass $\mathrm{Re}(E) = 17^{+4}_{-4}\,\mathrm{MeV}$ and a decay width $\Gamma = 112^{+90}_{-103}\,\mathrm{MeV}$.

Acknowledgements

We acknowledge useful conversations with K. Cichy. P.B. acknowledges the support of CFTP (grant FCT UID/FIS/00777/2013) and is thankful for hospitality at the Institute of Theoretical Physics of Johann Wolfgang Goethe-University Frankfurt am Main. M.C. acknowledges the support of CFTP and the FCT contract SFRH/BPD/73140/2010. M.W. acknowledges support by the Emmy Noether Programme of the DFG (German Research Foundation), grant WA 3000/1-1.

This work was supported in part by the Helmholtz International Center for FAIR within the framework of the LOEWE program launched by the State of Hesse. Calculations on the LOEWE-CSC and on the on the FUCHS-CSC high-performance computer of the Frankfurt University were conducted for this research. We would like to thank HPC-Hessen, funded by the State Ministry of Higher Education, Research and the Arts, for programming advice.

References

[1] W. Detmold, K. Orginos and M. J. Savage, *BB Potentials in Quenched Lattice QCD*, *Phys. Rev.* **D76** (2007) 114503 [hep-lat/0703009].

[2] ETM collaboration, M. Wagner, *Forces between static-light mesons*, *PoS* **LATTICE2010** (2010) 162 [1008.1538].

[3] QCDSF collaboration, G. Bali and M. Hetzenegger, *Static-light meson-meson potentials*, *PoS* **LATTICE2010** (2010) 142 [1011.0571].

[4] ETM collaboration, M. Wagner, *Static-static-light-light tetraquarks in lattice QCD*, *Acta Phys. Polon. Supp.* **4** (2011) 747 [1103.5147].

[5] P. Bicudo and M. Wagner, *Lattice QCD signal for a bottom-bottom tetraquark*, *Phys. Rev.* **D87** (2013) 114511 [1209.6274].

[6] Z. S. Brown and K. Orginos, *Tetraquark bound states in the heavy-light heavy-light system*, *Phys. Rev.* **D86** (2012) 114506 [1210.1953].

[7] P. Bicudo, K. Cichy, A. Peters, B. Wagenbach and M. Wagner, *Evidence for the existence of $ud\bar{b}\bar{b}$ and the non-existence of $ss\bar{b}\bar{b}$ and $cc\bar{b}\bar{b}$ tetraquarks from lattice QCD*, *Phys. Rev.* **D92** (2015) 014507 [1505.00613].

[8] P. Bicudo, K. Cichy, A. Peters and M. Wagner, *BB interactions with static bottom quarks from Lattice QCD*, *Phys. Rev.* **D93** (2016) 034501 [1510.03441].

[9] P. Bicudo, J. Scheunert and M. Wagner, *Including heavy spin effects in the prediction of a $\bar{b}\bar{b}ud$ tetraquark with lattice QCD potentials*, *Phys. Rev.* **D95** (2017) 034502 [1612.02758].

[10] A. Francis, R. J. Hudspith, R. Lewis and K. Maltman, *Doubly bottom strong-interaction stable tetraquarks from lattice QCD*, 1607.05214.

[11] P. Bicudo and M. Cardoso, *Tetraquark bound states and resonances in the unitary and microscopic triple string flip-flop quark model, the light-light-antiheavy-antiheavy $qq\bar{Q}\bar{Q}$ case study*, *Phys. Rev.* **D94** (2016) 094032 [1509.04943].

[12] P. Bicudo, M. Cardoso, A. Peters, M. Pflaumer and M. Wagner, *$ud\bar{b}\bar{b}$ tetraquark resonances with lattice QCD potentials and the Born-Oppenheimer approximation*, *Phys. Rev.* **D96** (2017) 054510 [1704.02383].

[13] M. Born and R. Oppenheimer, *Zur Quantentheorie der Molekeln*, *Annalen der Physik* **389** (1927) 457.

[14] Particle Data Group collaboration, K. A. Olive et al., *Review of Particle Physics*, *Chin. Phys.* **C38** (2014) 090001.

[15] E. Merzbacher, *Quantum Mechanics (3rd edition)*, *Wiley* (1998) .